Ductility of fiber-reinforced self-consolidating concrete under multi-axial compression

Alessandro P. Fantilli *, Paolo Vallini [1], Bernardino Chiaia [2]

Department of Structural and Geotechnical Engineering, Politecnico di Torino, Corso Duca degli Abruzzi 24, 10129 Torino, Italy

A B S T R A C T

The results of 12 multi-axial compression tests performed on cylinders made of self-consolidating concrete, plain (SCC) and reinforced with steel fibers (FR-SCC), are presented in this paper. In the experimental campaign, four "reference" confining pressures (0, 1, 3 and 10 MPa) were applied on the lateral surface of the specimens. After the first stage of loading, when a hydraulic stress was applied to the cylinders, and progressively increased up to the value of a pre-established confining pressure, a longitudinal compressive load was used to generate crushing of concrete. During this failure, the post-peak behavior of SCC and FR-SCC can be defined by a non-dimensional function that relates the inelastic displacement and the relative stress during softening. Such a function also reveals the ductility of SCC, which increases with the confinement stress and with the fiber volume fraction. In particular, by adding 0.9% in volume of steel fibers, FR-SCC can show practically the same ductility measured in unreinforced SCC with 1 MPa of confining pressure. Thus, the presence of an adequate amount of fibers in SCC columns is sufficient to create a sort of distributed confinement.

1. Introduction

The mechanical response and the ductility of reinforced concrete (RC) beams and columns, which fail via concrete crushing in compressed zones, depend on the type of concrete. This is the case, for instance, of over-reinforced concrete beams, like those in four point bending tested by Mansur et al. [1]. The post-peak behavior of fiber-reinforced concrete (FRC) beams is remarkably more ductile than that observed in beams having the same geometry, the same steel rebars, and the same bearing capacities, but made of normal vibrated concrete (NC) without fiber. Similarly, the experimental campaign conducted by Khayat et al. [2] on highly confined RC columns, subject to concentric compression, shows that the load vs. average axial strain diagrams appear more ductile in the case of columns made of self-compacting concrete (SCC), than in similar NC columns.

These experimental observations can be usefully applied to designing RC compressed columns in seismic regions. In fact, according to Eurocode 8 [3], if a required ductility cannot be attained because concrete strains are larger than 0.35%, a compensation for the loss of resistance due to crushing can be achieved by means of an adequate confinement. Such a confinement, usually guaranteed by transversal steel reinforcement (i.e., stirrups), can also be provided by FRC. In other words, short steel fibers randomly dispersed in a cement-based matrix can generate a sort of confining pressures comparable with that of stirrups, as confirmed by Ganesan's and Ramana Murthy's tests [4].

Although FRC has been introduced to increase the ductility of cement-based composites in tension [5], and SCC to avoid concrete vibration [6], they can together provide a sort of confinement, and therefore higher ductility in compression. As a result, their combination can bring to remarkable advantages in reducing the amount of ordinary reinforcement. In particular, higher strength and larger ultimate strain have been measured in confined columns made with steel fibers and self-consolidating concrete (FR-SCC) columns [7].

The equivalent confinement produced by the fiber-reinforcement cannot be easily quantified by the classical tests on columns, because the contribution of fibers cannot be separated from that of transverse reinforcement, and from the concrete matrix as well. Moreover, as observed in several tests [2,4,7], passive confinement provided by stirrups is only activated by the dilation of concrete. Thus, to obtain the stress–strain relationship under multi-axial compression, the axial stress–lateral strain of concrete must be defined in advance [8]. Conversely, in the case of active

Nomenclature

a, b	coefficients of $F(w)$ (Eq. (4))
A_c	$d_1 \cdots d_2$ = cross-sectional area of a column
A_F	area defined by the function $F(w)$
$A_{F,min}$, $A_{F,max}$	minimum and maximum values of A_F
$A_{s,l}$	cross-sectional area of the longitudinal reinforcing bars in RC column
$A_{s,s}$	cross-sectional area of stirrups in RC column
c_f	concrete cover in RC column
D	diameter of cylindrical specimen under compression
d_1, d_2	cross-section dimensions of rectangular RC column
d_b	diameter of longitudinal rebar in RC column
d_c	dimension of the core area in RC column
d_s	diameter of stirrups in RC column
E_c	Young's modulus of a cement-based material
f_c	compressive strength of a cement-based material
f_{ct}	tensile strength of a cement-based material
f_y	yielding strength of steel rebar
$F(w) = \sigma_c/f'_c$	relative stress in the post-peak stage of a cement-based material in compression
H, ΔH	height of a cylindrical specimen (and its decrement)
L/Φ	fiber aspect ratio (L = length of a fiber; Φ = diameter of a fiber)
n	number of stirrups legs in RC column
P	compressive load applied on a cylindrical specimen
s	sliding displacement in concrete specimens due to crushing (Fig. 1a)
s_s	spacing between stirrups in RC column
RI	$V_f \cdot L/\Phi$ = reinforcing index
V_f	fiber volume fraction
w	inelastic displacement in compression
α	angle between the sliding plane and the direction of applied loads in a cement-based material in compression
ε_c	compressive strain in a cement-based material
$\varepsilon_{c,el}$	residual strain corresponding to a stress decrement during softening (Fig. 1b)
ε_{c1}	compressive strain at maximum stress of a cement-based material
σ_3	confining pressure
σ_c, $\Delta\sigma_c$	compressive stress in a cement-based material (and its decrement)

confinement, it is not necessary to know the concrete swelling, because confining pressure, applied on cubes (in one or two directions) or cylinder (in triaxial tests), is directly controlled by the operator [9].

In the past years, triaxial tests were generally used to measure the strength of concrete under multi-axial compression, including the size effect of high strength concrete [10]. Only recently, fiber-reinforced concrete (and in particular high performance fiber-reinforced cementitious composites – HPFRCC) has been tested in multi-axial compression in order to investigate the role of fiber content in the post-peak response [11]. In this case, however, reinforcement has never been considered as an applied confinement. Thus, with the aim of quantifying the equivalent confinement that can be activated by fiber-reinforcement, a new experimental campaign, performed on SCC cylinders in uniaxial and triaxial compression, is herein described.

2. The post-peak response of compressed concrete

As the ductility of different cement-based composites has to be taken into consideration, the crushing failure of concrete in compression needs to be properly defined. The stress–strain relationship σ_c–ε_c of cement-based materials in compression (Fig. 1a) can be divided into two parts (Fig. 1b). In the first part, when the stress is lower than the strength f_c (and $\varepsilon_c < \varepsilon_{c1}$), strain localization does not appear, even though the specimen can show diffuse internal cracking (or distributed damage). In the case of plain concrete, the ascending branch of σ_c–ε_c can be univocally defined by the Sargin relationship [12]. As soon as the peak stress is reached, localized damage develops and strain softening begins [9]. In this stage, there is the formation of either a system of longitudinal cracks (parallel to the applied load) or an inclined crack band, which subdivides the specimen into two progressively-sliding blocks. In the latter case (Fig. 1c), the angle between the vertical axis of the specimen and the sliding surfaces is assumed to be $\alpha = 18°$, as experimentally measured by Fujita et al. [13]. Moreover, according to the Mohr–Coulomb failure criterion, this value is more or less the inclination of the failure surface when tensile strength is assumed to be 1/10 of compressive strength ($f_{ct} = 0.1 f_c$). The inelastic displacement w of the specimen, and the consequent sliding s of the blocks along the sliding surface, are the parameters governing the average post-peak compressive strain ε_c of the specimen (Fig. 1).

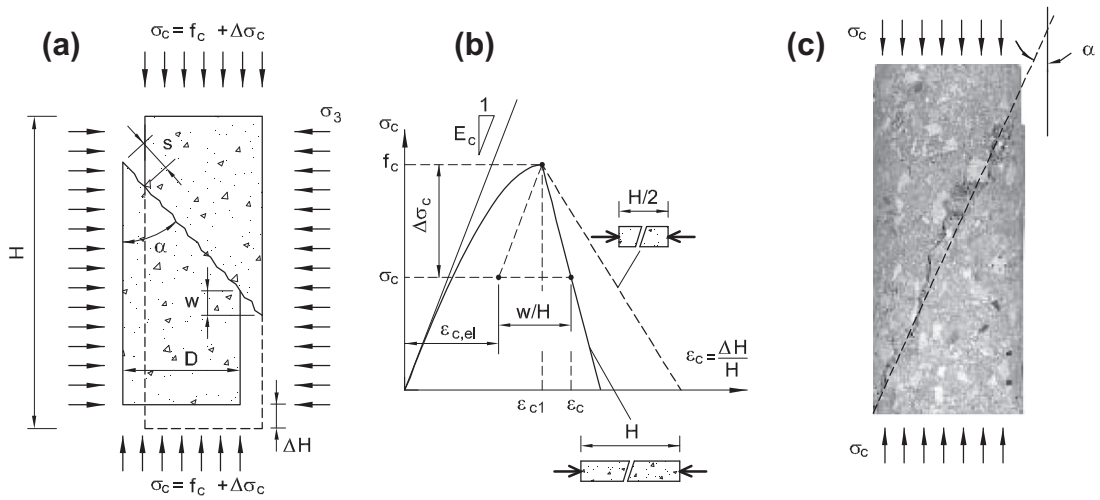

Fig. 1. The post-peak response of compressed concrete: (a) the kinematic variables involved in the softening branch; (b) the complete stress–strain relationship; (c) onset of strain localization.

Referring to the specimen depicted in Fig. 1a, post-peak strains can be defined by the following equation [9]:

$$\varepsilon_c = \varepsilon_{c,el} + \frac{w}{H} = \varepsilon_{c1} - \frac{\Delta\sigma_c}{E_c} + \frac{w}{H} \quad (1)$$

where ε_{c1} is the strain at compressive strength f_c (assumed to be positive); $\Delta\sigma_c$ is the stress decrement after the peak and H is the height of the specimen.

Due to the w/H ratio involved in the evaluation of ε_c (Eq. (1)), and according to test measurements [9,14], longer specimens behave in a more brittle manner, as the post-peak slope of σ_c–ε_c increases in longer specimens (see Fig. 1b). The stress decrement $\Delta\sigma_c$ can be defined as:

$$\Delta\sigma_c = f_c - \sigma_c = f_c \cdot [1 - F(w)] \quad (2)$$

where $F(w)$ is the non-dimensional function which relates the inelastic displacement w and the relative stress σ_c/f_c during softening.

Substituting Eq. (2) into Eq. (1), it is possible to obtain a new equation for ε_c:

$$\varepsilon_c = \varepsilon_{c1} - \frac{f_c \cdot [1 - F(w)]}{E_c} + \frac{w}{H} \text{ for } \varepsilon_c > \varepsilon_{c1} \quad (3)$$

Eq. (3), adopted for the post-peak stage of a generic cement-based material in compression, is based on the definition of $F(w)$, assumed to be a material property [9,14]. In the considered cement-based composites, this function should be evaluated experimentally on cylindrical specimens, as performed by Jansen and Shah [14] for plain concrete.

Fig. 2a shows the $F(w)$ relationships proposed by Fantilli et al. [15], which consists of two parabolas and a constant branch:

$$F(w) = \frac{\sigma}{f_c} = 1 + a \cdot w^2 + b \cdot w \quad \text{for } 0 \leqslant w \leqslant -\frac{b}{2 \cdot a} \quad (4a)$$

$$F(w) = \frac{\sigma}{f_c} = -\left(1 - \frac{b^2}{4 \cdot a}\right) \cdot \left(\frac{4 \cdot a^2}{b^2} w^2 + \frac{4 \cdot a}{b} w\right) \quad \text{for } -\frac{b}{2 \cdot a} < w \leqslant -\frac{b}{a} \quad (4b)$$

$$F(w) = \frac{\sigma}{f_c} = 0 \quad \text{for } w > -\frac{b}{a} \quad (4c)$$

The parabolas are both defined by the same coefficients a, b and have the same extreme point at $w = -0.5b/a$, whereas $w = -b/a$ (i.e. twice the value at extreme point) is considered the maximum inelastic displacement corresponding to $F(w)$ larger than zero.

In the case of the NC specimens, the values $a = 0.320\ \text{mm}^{-2}$ and $b = -1.12\ \text{mm}^{-1}$ were obtained by means of the least square approximation of several tests [15]. As observed in Fig. 2b, the curves defined by Eq. (4) fall within the range of the data experimentally measured by Jansen and Shah [14].

Analogously to concrete in tension [16], the area A_F of the $F(w)$ curve (Fig. 2a) can be considered as proportional to the work of fracture in compression, and can be used to measure the ductility of the investigated materials.

3. Experimental program

The post-peak behavior of cement-based composites in compression has been investigated at the Department of Structural and Geotechnical Engineering of Politecnico di Torino (Italy) by means of uniaxial and triaxial tests on SCC and FR-SCC cylinders (Fig. 3). The experimental equipment, named HTPA (High Pressure Triaxial Apparatus) and described by Chiaia et al. [12], is generally used to test cylindrical specimens made of soft rocks.

Each triaxial test consists of two stages. A specimen is initially loaded by a hydrostatic pressure (which coincides with the pre-established confining pressure σ_3 – Fig. 3b), then the load P is applied along the longitudinal direction with a velocity of 37 μm per minute (Fig. 3c). During the second stage of loading, the pressure $\sigma_3 = const.$ is applied to the lateral surface, whereas the longitudinal nominal stress σ_c becomes:

$$\sigma_c = \sigma_3 + \frac{4P}{\pi D^2} \quad (5)$$

where P is the applied load and D is the diameter of the cross-section.

Through a couple of LVDT, the local longitudinal displacements, and therefore the nominal longitudinal strains ε_c, are also measured (Fig. 3a).

Four confining pressures, namely $\sigma_3 = 0$, 1, 3, and 10 MPa, have been applied to the specimens. During the application of hydrostatic loads (Fig. 3b), stress increments are electronically recorded every 10 s. Similarly, in the second stage, when $\sigma_3 = const.$ and P increases, the values of the applied load, the relative displacement between the specimen's ends, and the longitudinal displacement along the lateral surface (taken by the LVDTs of Fig. 3a) are measured.

Three series of specimens, each composed by four cylinders (of height $H = 140$ mm and diameter $D = 70$ mm), were made with the SCC reported in Table 1. Dramix RC 65/35 BN steel fibers (length $L = 35$ mm, diameter $\Phi = 0.55$ mm) having hooked ends were added to the specimens of Series 2 and Series 3 in the proportions of 35 kg/m^3 (volume fraction $V_f = 0.45\%$) and 70 kg/m^3 ($V_f = 0.9\%$,), respectively. In the first case, the reinforcing index RI (i.e., the product of the fiber volume fraction V_f and the fiber aspect ratio L/Φ) was 28.8%, whereas in the latter case $RI = 57.6\%$.

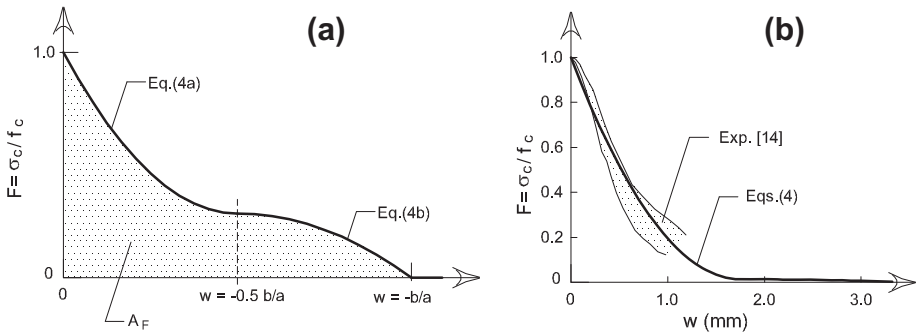

Fig. 2. The $F(w)$ curves of normal vibrated concrete: (a) the relationship proposed by Fantilli et al. [15]; (b) the experimental curves measured by Jansen and Shah [14].

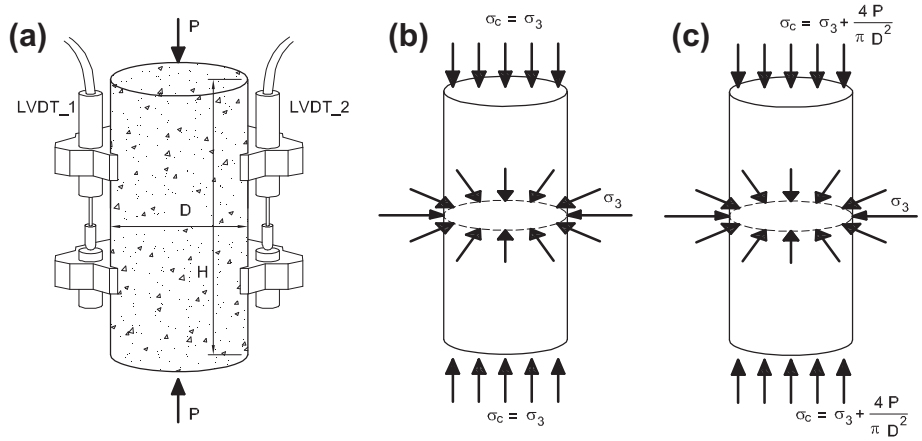

Fig. 3. The two stages of loading in the triaxial tests: (a) locations of the LVDTs; (b) the confining pressure; (c) application of the longitudinal load *P*.

Table 1
Composition and strength of self-consolidating concrete.

Constituents	kg/m^3
Water	180
Superplasticizer (Addiment Compactcrete 39/T100)	4.49
Cement (Buzzi Unicem II/A-LL 42.5 R)	250
Carbonate filler (Nicem Carb VG1-2)	380
Fine aggregate (0–4 mm)	910
Coarse aggregate (6.3–12 mm)	600
Cubic strength (MPa)	30.4

Table 2
The cylindrical specimens tested in uniaxial and triaxial compression.

Series	Specimen	Steel fibers (kg/m^3)	σ_3 (MPa)
1	0SC0	0	0
	0SC1	0	1
	0SC3	0	3
	0SC10	0	10
2	35SC0	35	0
	35SC1	35	1
	35SC3	35	3
	35SC10	35	10
3	70SC0	70	0
	70SC1	70	1
	70SC3	70	3
	70SC10	70	10

The specimens of each series had the same geometry (D = 70 mm, H = 140 mm), were cast simultaneously in polystyrene form, then cured for one week under identical laboratory conditions, and finally tested one month later. The characteristics of the specimens are reported in Table 2, where they are also named with an alphanumeric acronym. On the left side of the letters SC, the kilograms (0, 35, 70) of steel fibers added to each cubic meter of self-consolidating concrete are reported, whereas the number on the right side indicates the value of confining pressure (0, 1, 3, 10 MPa).

4. Experimental results

Fig. 4 reports the stress–strain curves obtained from the specimens of Series 1 (Fig. 4a), Series 2 (Fig. 4b) and Series 3 (Fig. 4c). The higher the confinement, the higher the values of f_c and ε_{c1}, which are reported, together with Young's modulus, E_c, in Table 3. In all the cases, after the peak stress f_c, a remarkable strain softening branch can be observed in the σ_c–ε_c diagrams.

Although the specimens of Series 2 and Series 3 are fiber-reinforced, the compressive strength, measured at all the applied σ_3, does not differ substantially from that of SCC (Series 1). The same results can be also obtained for normal concrete under tensile actions [5], whose strength remains unchanged if the fiber volume fraction is lower than 1% (as in the present test campaign).

The post-peak response of FR-SCC composites appears more ductile with the increase of the fiber volume content. By comparing the softening branches of the σ_c–ε_c curves reported in Fig. 4, it seems that the post-peak response of the specimens 0SC1 and 0SC3 (Series 1) is more or less the same of the specimens 70SC0 and 70SC1 (Series 3), respectively. However, for a low fiber content (i.e., V_f = 0.45% of Series 2), neither the strength nor the ductility of SCC increase. Thus, in these situations, the cost of adding fibers is not justified by the deriving benefits. Conversely, the ductility of SCC increases with the confining pressure. For σ_3 = 10 MPa, the stress–strain curves of self-consolidating concrete show a pseudo-plastic post-peak response, regardless of the fiber content (compare, e.g., the curves of the specimens 0SC10, 35SC10, and 70SC10 reported in Fig. 4). According to Sirijaroonchai et al. [11], also for High Performance Concretes, the confining effect produced by fibers reduces in presence of high confining pressure.

4.1. Post-peak comparison in terms of F(w) and AF

As both strain localization and diagonal cracks occurred in all triaxial tests (see the photos of the specimens 0SC1, 35SC1 and 70SC1 reported in Fig. 5), the post-peak stage of SCC and FR-SCC can be described, for all the length and the strength values of the specimens, by the $F(w)$ curves, and by the areas A_F, as previously defined. Specifically, for a given $\varepsilon_c > \varepsilon_{c1}$, the decrease of compressive stress $\Delta\sigma_c = f_c - \sigma_c$ (and $F = \sigma_c / f_c$) can be obtained through the σ_c–ε_c curves reported in Fig. 4, whereas the corresponding w (Fig. 1a) can be computed by Eq. (3) (f_c, ε_{c1}, E_c and H are known from the tests).

The $F(w)$ curves are reported in Figs. 6a, 7a and 8a for the specimens of the Series 1, Series 2, and Series 3, respectively. In the same figures, the dashed curves represent the behavior of NC as predicted by Eq. (4) in the case of zero confinement. All the curves are limited to w = 4 mm, in correspondence of which residual compressive stresses vanish in normal vibrated concrete, as confirmed both by the present test and by the predictive model (Eq. (4) in

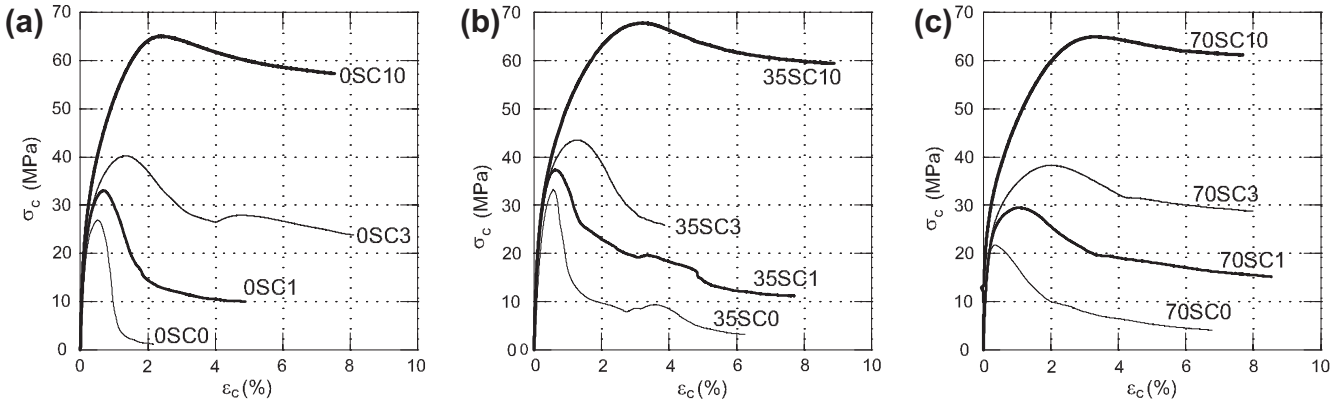

Fig. 4. The σ_c–ε_c curves resulting from triaxial tests: (a) Series 1; (b) Series 2; (c) Series 3.

Table 3
Main mechanical properties measured in the tests.

Series	Specimen	f_c (MPa)	ε_{c1}	E_c (MPa)
1	0SC0	26.3	0.00513	25,000
	0SC1	32.0	0.00696	27,000
	0SC3	40.3	0.0135	27,000
	0SC10	65.1	0.0245	35,000
2	35SC0	34.5	0.00611	25,000
	35SC1	37.3	0.00629	27,000
	35SC3	42.5	0.0125	28,000
	35SC10	67.8	0.0326	30,000
3	70SC0	21.8	0.00352	18,000
	70SC1	29.5	0.0109	20,000
	70SC3	38.3	0.0207	26,000
	70SC10	64.9	0.0339	42,000

Fig. 6a). Although FR-SCC can show remarkable residual stresses even at $w > 4$ mm, they can hardly reach such deformation in practice, because at this value of w a NC or SCC specimen (or column) is completely crushed.

Only the behavior of the specimen 0SC0 is correctly predicted by Eq. (4) (Fig. 6a). Whereas, in the absence of confining pressures, the slope of $F(w)$ decreases with the increase of fiber volume fraction (compare the difference between the curves of the Specimens 0SC0, 35SC0, and 70SC0 with that of Eq. (4) in Figs. 6a, 7a and 8a, respectively). A very ductile response can also be achieved by increasing the confining pressure, as shown by the specimens 0SC10, 35SC10 and 70SC10, whose $F(w)$ curves reveal a pseudo-plastic behavior, independently of fiber content.

Within the observed range ($w \sim 0$–4 mm), the ductility in compression can be objectively measured by the area A_F under the curve $F(w)$:

$$A_F = \int_0^{4\text{mm}} F(w)dw \tag{6}$$

As $F(w)$ is the relative stress normalized with respect to the compressive strength f_c, the comparison between all the tested cement-based composites, under uniaxial and multi-axial compression, is possible. Higher values of A_F are attained in a concrete capable of maintaining high loads after failure (i.e., in the case of high ductility materials). Obviously, the maximum ductility $A_{F,max} = 4$ mm is reached in the case of plastic behavior [$F(w) = 1 = const.$], whereas the minimum ductility is that of normal vibrated concrete. To be more precise $A_{F,min} = 0.61$ mm, is obtained by substituting Eq. (4) (with $a = 0.320$ mm^{-2} and $b = -1.12$ mm^{-1}) into Eq. (6). Both the values of $A_{F,max}$ and $A_{F,min}$ are evidenced in the histograms of Figs. 6b, 7b and 8b, where the measured values A_F of the Series 1, Series 2, and Series 3 are respectively reported.

In all the cases, A_F is between $A_{F,max}$ and $A_{F,min}$, the latter corresponding to the normal and self-consolidating concrete without any confinement. Nevertheless, at $\sigma_3 = 0$, the lower limit is approximately attained for the specimens of Series 1 and Series 2 ($A_F = 0.75$ mm for the Specimen 0SC0, and $A_F = 0.88$ mm for the Specimen 35SC0), whereas the Specimens 70SC0 (Series 3) shows a value three times higher ($A_F = 2.37$ mm). The upper limit is generally reached for high confining pressure ($\sigma_3 = 10$ MPa), regardless of the fiber volume fraction ($A_F = 3.81$ mm for the

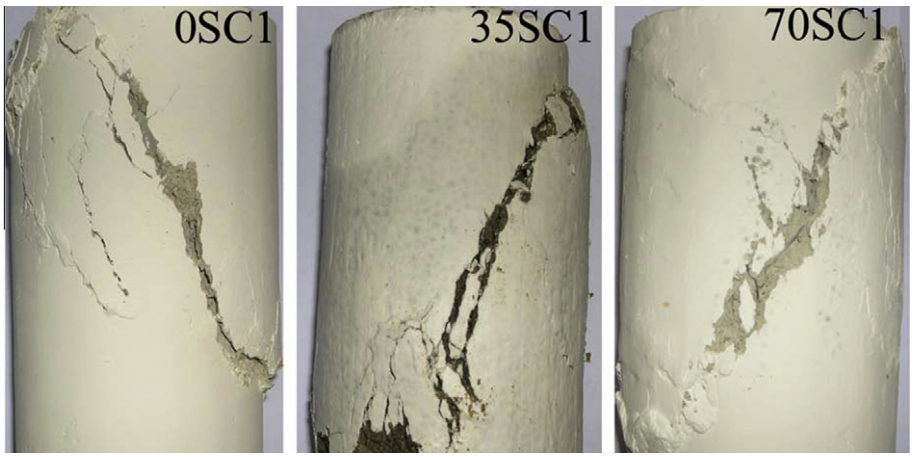

Fig. 5. The diagonal failure in the specimens 0SC1, 35SC1, and 70SC1.

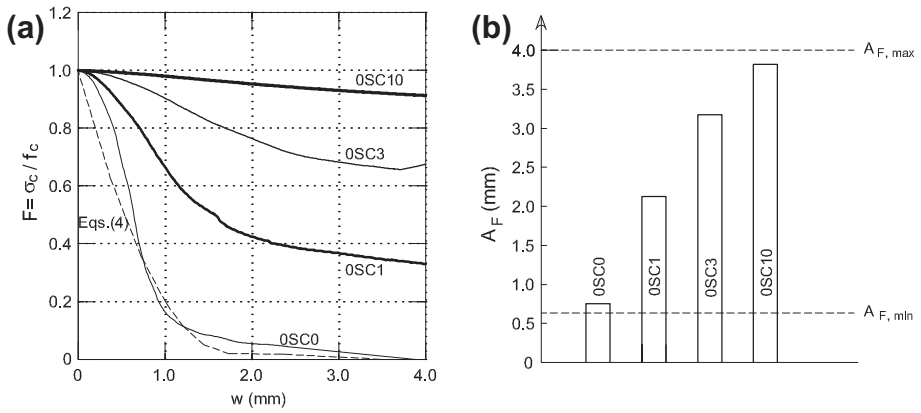

Fig. 6. The post-peak response of the specimens made of plain SCC (Series 1): (a) $F(w)$ curves; (b) histogram of the areas A_F measured in the tests.

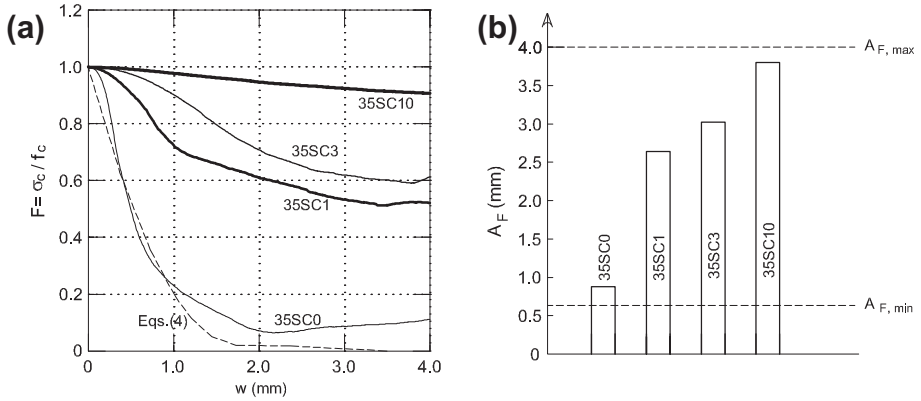

Fig. 7. The post-peak response of the specimens made of SCC + 35 kg/m^3 of steel fibers (Series 2): (a) $F(w)$ curves; (b) histogram of the areas A_F measured in the tests.

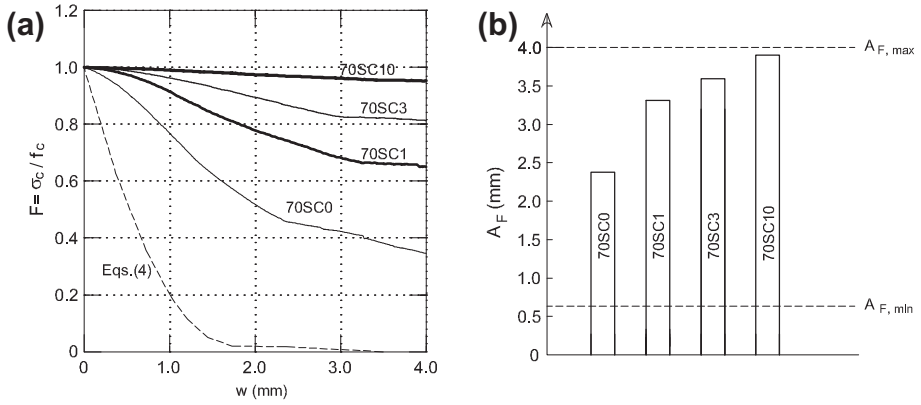

Fig. 8. The post-peak response of the specimens made of SCC + 70 kg/m^3 of steel fibers (Series 3): (a) $F(w)$ curves; (b) histogram of the areas A_F measured in the tests.

Specimen 0SC10, $A_F = 3.8$ mm for the Specimen 35SC10, and $A_F = 3.9$ mm for the Specimen 70SC10). In other words, for each series, the difference between the maximum (corresponding to $\sigma_3 = 10$ MPa) and the minimum (corresponding to $\sigma_3 = 0$) values of A_F decreases with the fiber volume fraction. For this reason, steel fibers can effectively guarantee a sort of confinement, especially for the FR-SCC of Series 3 at low confining pressures ($\sigma_3 = 0$–1 MPa).

5. The equivalent confinement of FR-SCC

As evidenced by the $F(w)$ curves reported in Fig. 9, the equivalent confinement produced by steel fibers, already observed by Ganesan and Ramana Murthy [4] and by Aoude et al. [7], can be really significant in the case of high fiber volume fraction. Specifically, in Fig. 9a the curves of the specimens 70SC0 and 35SC0 are reported, which are fiber-reinforced and subjected to uniaxial compression. The same Figure reports the curves of the specimen 0SC1 tested in triaxial compression ($\sigma_3 = 1$ MPa). As a reference, the $F(w)$ curve given by Eq. (4), which describes the post-peak behavior of plain NC and SCC under uniaxial compression, is also depicted in Fig. 9a. Only the presence of 70 kg/m^3 of steel fibers in the SCC of Table 1 can provide a sort of confinement equal to 1 MPa, as confirmed by the close proximity of the $F(w)$ curves obtained from the specimens 70SC0 and 0SC1 (Fig. 9a). Conversely, an amount of fibers lower than 35 kg/m^3 of SCC (Specimens 35SC0 in Fig. 9a) does not change substantially the post-peak response of plain concrete (Eq. (4) in Fig. 9a).

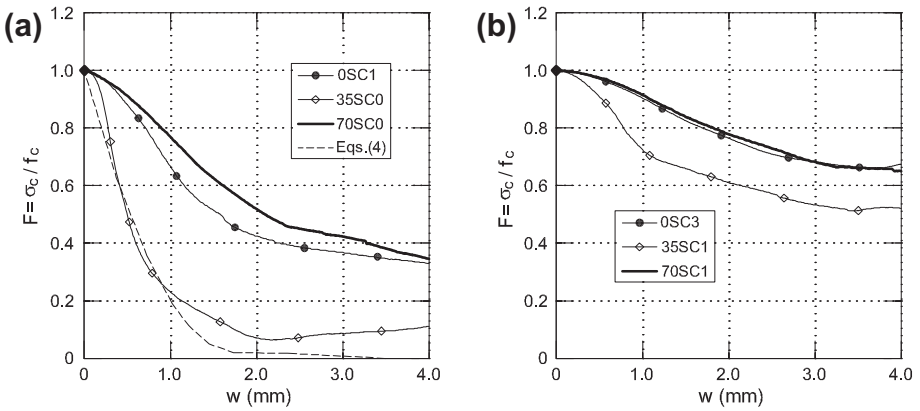

Fig. 9. The equivalent confinement in FR-SCC: (a) the $F(w)$ relationships of the specimens 0SC1, 35SC0, and 70SC0; (b) the $F(w)$ relationships of the specimens 0SC3, 35SC1, and 70SC1.

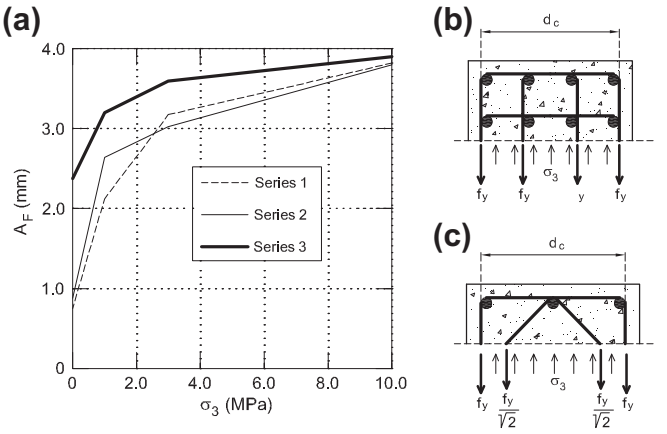

Fig. 10. The ductility of SCC as a function of confining pressures and fiber volume fraction: (a) the curves A_F–σ_3 measured for the three series of SCC; (b) and (c) calculation of confining pressures in some RC columns [17].

Analogously, Fig. 9b reports the $F(w)$ curve of the specimen 70SC1 (tested at $\sigma_3 = 1$ MPa), which matches that of the Specimen 0SC3 (tested at $\sigma_3 = 3$ MPa). Thus, the FR-SCC of Series 3 (in which 70 kg/m^3 of steel fibers are added to the SCC of Table 1), confined at 1 MPa, can show the same ductility of plain SCC subjected to a confining pressure $\sigma_3 = 3$ MPa.

The confining effects of fibers, as measured in the uniaxial and triaxial tests carried out on the specimens listed in Table 2, are summarized in Fig. 10a. For the three fiber volume contents (respectively, 0 kg/m^3 for the specimens of Series 1, 35 kg/m^3 for the specimens of Series 2, and 70 kg/m^3 for the specimens of Series 3), the curves A_F *vs.* the confining pressures σ_3 are depicted in Fig. 10. With respect to plain SCC, the presence of 35 kg/m^3 of steel fibers does not modify substantially the ductility of normal and self-consolidating concrete. A dramatic increment of A_F can only be observed in the specimens of Series 3 (70 kg/m^3 of steel fibers), particularly for the lower confining pressures.

From the practical point of view, the diagrams of Fig. 10a can be used to design the transversal reinforcement of concrete columns. During the failure stage, such reinforcement, generally made of steel stirrups, can provide a sort of confinement and thus increase the ductility of compressed members. As shown in Fig. 10b and c, the value of confining pressure σ_3 depends on the column cross-section [15], and can generally be computed by the following equation:

$$\sigma_3 = \frac{nA_{s,s}f_y}{d_c s_s} \tag{7}$$

where n is number of stirrups legs ($n = 4$ for the cross-section depicted in Fig. 10b, whereas $n = 2(1 + 1/\sqrt{2})$ for the cross-section depicted in Fig. 10c); $A_{s,s}$ = cross-section of stirrup; f_y = yielding strength of stirrup; d_c = one of the dimensions of the so-called core area, which is the area inside the perimeter of stirrup; s_s = spacing between stirrups.

According to Eurocode 2 [18], in concrete columns a minimum amount of reinforcement has to be arranged both longitudinally and transversally. Specifically, the cross-sectional area $A_{s,l}$ of the longitudinal reinforcing bars (of diameter $d_b \geqslant 6$ mm) should be comprised between the following limits:

$$0.002A_c \leqslant A_{s,l} \leqslant 0.08A_c \tag{8}$$

where A_c is $d_1 d_2$ = cross-sectional area of the column.

The spacing s_s of the transverse reinforcing bars, having a diameter $d_s \geqslant 6$ mm or $d_s \geqslant 0.25\, d_b$, should be equal to, or lower than the least value between 20 times d_b, 400 mm and the minimum between d_1 and d_2. In some cases (e.g., near the lap joints) the maximum required spacing should be reduced by a factor 0.6.

All the above-mentioned conditions are satisfied by the Column 1 depicted in Fig. 11a, whose geometrical and mechanical properties are indicated in Table 4. If subjected to axial compression, the stirrups of such a column can generate a confining pressure $\sigma_3 = 1.4$ MPa (Eq. (7), $n = 2$). In the case of Column 1 made by plain SCC (i.e., that of Series 1), such a confinement leads to a value $A_F = 2.4$ mm (point A in Fig. 11c). The same ductility (point B in Fig. 11c) provided by the Column 2 (Fig. 11b, Table 4) made by the same SCC and 70 kg/m^3 of steel fibers (i.e., the concrete of Series 3), without any stirrups ($\sigma_3 = 0$). Indeed, Fig. 11 clearly shows the better performances of columns made by FR-SCC, in which steel fibers provide an effective confinement. In other cases, such as the nodes of RC frames subjected to heavy seismic loads, reduction of stirrups, and consequently of rebar congestion, can economically justify the use of more expensive fiber-reinforced composites. Moreover, with respect to the classical stirrups, capable of generating a passive confinement within the core area, the beneficial effect of fibers is more effectively distributed, and comparable to a confining pressure spread inside the whole column.

6. Conclusions

From the results of an experimental campaign performed on SCC cylinders, with and without steel fibers and subjected to uniaxial and multi-axial compression, the following conclusions can be drawn:

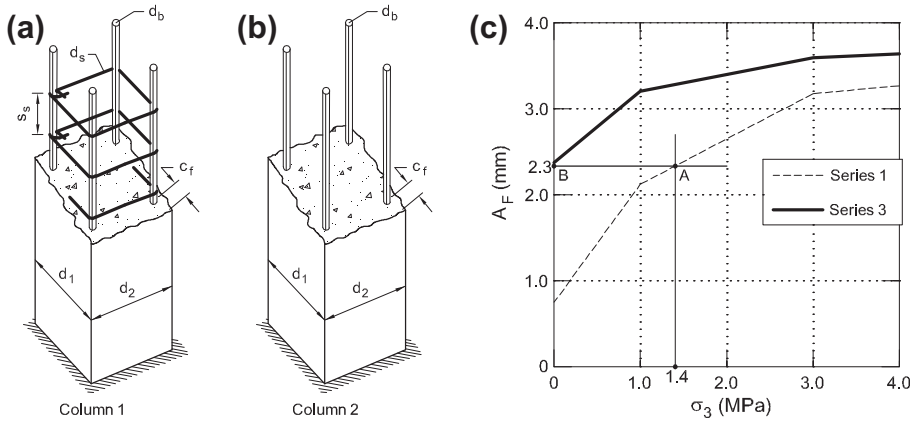

Fig. 11. The confinement in RC columns: (a) the Column 1 made of SCC (Series 1) and transversally reinforced in accordance with Eurocode 2 [18]; (b) the Column 2 made of SCC + 70 kg/m^3 of steel fibers (Series 3) without stirrups; (c) the equivalence between the values of A_F as evidenced by the triaxial tests.

Table 4
Geometrical and mechanical properties of Column 1 (Fig. 11a) and Column 2 (Fig. 11b).

	Column 1	Column 2
d_1 (mm)	300	300
d_2 (mm)	300	300
d_b (mm)	16	16
d_s (mm)	10	–
s_s (mm)	180	–
c_f (mm)	20	20
f_y (MPa)	450	450

- In self-consolidating concrete, the ductility in compression increases with active confinement, and/or with the fiber volume fraction. Nevertheless, for low fiber content (less than 0.45%), no benefit is evident, both in terms of strength and ductility.
- During the post-peak stage, the ductility SCC with 70 kg/m^3 of steel fibers is comparable with that of SCC at 1 MPa of confining pressure made by stirrups.
- Under compression, the performance of fiber-reinforced composites can be quantified by the distributed confining pressure generated by the fibers.
- As theoretical principle, all the previous observations can be applied to RC columns made with FR-SCC. For such structures, the beneficial effect of fibers can be comparable with that of a confining pressure applied along the column.

Finally, the presence of a confinement can improve the ductility of concrete and, consequently, its durability. However, further tests will be developed in full-scale RC columns in order to verify the higher ductility of real structures made of FR-SCC.

Acknowledgments

The authors wish to express their gratitude to Fondazione Cassa di Risparmio di Alessandria for financing this research work, and to Buzzi Unicem S.p.A. for the technical support.

References

[1] Mansur MA, Chin MS, Wee TH. Flexural behaviour of high-strength concrete beams. ACI Struct J 1997;94(6):663–74.
[2] Khayat KH, Paultre P, Tremblay S. Structural performance and in-place properties of self-consolidating concrete used for casting highly reinforced columns. ACI Mater J 2001;98(1):371–8.
[3] UNI EN 1998-1. Eurocode 8 – design of structures for earthquake resistance – part 1: general rules, seismic actions and rules for buildings. Reported by CEN; 2005.
[4] Ganesan N, Ramana Murthy JV. Strength and behaviour of confined steel fiber reinforced concrete columns. ACI Mater J 1990;87(3):221–7.
[5] Balaguru N, Shah SP. Fiber reinforced cement composites. New York: McGraw Hill; 1992.
[6] Okamura H, Ouchi M. Self-compacting concrete. J Adv Conc Technol 2003;1(1):5–15.
[7] Aoude H, Cook WD, Mitchell D. Behavior of columns constructed with fibers and self-consolidating concrete. ACI Struct J 2009;106(3):349–57.
[8] Lokuge WP, Sanjayan JG, Setunge S. Stress–strain model for laterally confined concrete. ASCE J Mater Civ Eng 2005;17(6):607–16.
[9] van Mier JGM. Fracture processes of concrete: assessment of material parameters for fracture models. Boca Raton: CRC Press; 1997.
[10] Li Q, Ansari F. High-strength concrete in triaxial compression by different sizes of specimens. ACI Mater J 2000;97(6):684–9.
[11] Sirijaroonchai K, El-Tawil S, Parra-Montesinos G. Behavior of high performance fiber reinforced cement composites under multi-axial compressive loading. Cem Concr Compos 2010;32(1):62–72.
[12] Chiaia B, Fantilli AP, Vallini P. Stress–strain relationship for steel fiber-reinforced self-consolidating concrete under multiaxial compression. Politecnico di Milano, Stud Res 2009;29:11–36.
[13] Fujita Y, Ishimaru R, Hanai S, Suenaga Y. Study on internal friction angle and tensile strength of plain concrete. In: Proceedings of fracture mechanics of concrete structures FRAMCOS 3. Freiburg, Germany: Aedificatio Publishers; 1998. p. 325–34.
[14] Jansen DC, Shah SP. Effect of length on compressive strain softening of concrete. ASCE J Eng Mech 1997;123(1):25–35.
[15] Fantilli AP, Mihashi H, Vallini P. Post-peak behaviour of cement-based materials in compression. ACI Mater J 2007;104(5):501–10.
[16] Hillerborg A, Modeer M, Peterson P. Analysis of crack formation and crack growth in concrete by means of fracture mechanics and finite elements. Cem Concr Res 1976;6(6):773–82.
[17] Foster SJ, Liu J, Sheikh SA. Cover spalling in HSC columns loaded in concentric compression. ASCE J Struct Eng 1998;124(12):1431–7.
[18] UNI EN 1992-1-1. Eurocode 2 – design of concrete structures – part 1-1: general rules and rules for building. Reported by CEN; 2005.